Available online at www.sciencedirect.com
SCIENCE DIRECT®
Chemical Physics Letters 409 (2005) 144–148
CHEMICAL PHYSICS LETTERS
www.elsevier.com/locate/cplett

On the energy transfer from nanocrystalline ZnS to Tb^{3+} ions confined in reverse micelles

Li Chen [a,c], Jiahua Zhang [a,*], Shaozhe Lu [a], Xinguang Ren [a], Xiaojun Wang [a,b,*]

[a] *Key Laboratory of Excited State Processes, Changchun Institute of Optics, Fine Mechanics and Physics, Chinese Academy of Sciences, 16 Eastern South-Lake Road, Changchun 130031, PR China*
[b] *Department of Physics, Georgia Southern University, Statesboro, GA 30460, USA*
[c] *Graduate School of the Chinese Academy of Sciences, Changchun, People's Republic of China*

Received 20 December 2004; in final form 11 April 2005
Available online 31 May 2005

Abstract

ZnS nanoparticles with different sizes are synthesized using a reverse micelles method in the presence of Tb^{3+} ions. The photoluminescence, excitation and absorption spectra of ZnS/Tb^{3+} NPs are studied to elucidate remarkable energy transfer from both ZnS host and the surfactant, i.e., AOT, to Tb^{3+} ions. When Tb^{3+} ions are introduced merely on the outside of ZnS nanoparticles in reverse micelles, obvious energy transfer from ZnS to the Tb^{3+} ions is also observed, indicating the important role of spatial confinement on the performance of energy transfer between host and luminescent centers which are even not doped into the host lattices.

1. Introduction

The photoluminescence (PL) properties of nanocrystalline II–IV semiconductors doped with 3d transition metal and rare earth (RE) ions have attracted much attention in both basic and applied research field during this decade [1–15]. RE ions-doped nanocrystalline semiconductors is expected to form a new luminescent materials with widely application such as on the optoelectronic devices because of the special sharp lines from the intra-shell 4f transitions of RE ions [14]. In addition, it was reported that RE ions especially Tb^{3+}/Eu^{3+} could be possibly used as sensitive luminescent probes in biomolecular system [16–18], and nanometer-sized semiconductors such as CdSe/ZnS were investigated intensively in respect of biological applications [19,20]. Promising widely application of such materials can be anticipated if the combination of the RE ions and semiconductor nanoparticles (NPs) is achieved.

Compared to the easiness of doping Mn^{2+} into ZnS host in nanometer regime [1,11,21,22], trivalent ions of rare earth have much difficulty to be incorporated into the ZnS NPs although it has been reported that RE ions can be doped into the bulk semiconductors as efficient activators, producing luminescence via $4f^n - 4f^n$ transitions [23–25]. A few papers, to the best of our knowledge, reported on the synthesis and luminescence properties of RE^{3+}-doped ZnS NPs, however, rare of them exhibits adequate evidence of energy transfer between ZnS host and RE^{3+} ions activators. This Letter is focused on the energy transfer between ZnS NPs and RE ions.

Although the surface of NPs generally plays a negative role on luminescence, we found that just on the surface of NPs, remarkable energy transfer occurs between ZnS host and Tb^{3+} ions. For the materials synthesized by conventional methods such as precipitation method, energy transfer from the host to the RE^{3+} is very difficult

* Corresponding authors. Fax: +86 431 6176317.
E-mail addresses: samsonciomp2000@yahoo.com (L. Chen), zjiahua@public.cc.jl.cn (J. Zhang).

0009-2614/$ - see front matter © 2005 Elsevier B.V. All rights reserved.
doi:10.1016/j.cplett.2005.04.106

to be observed because the RE ions are freely distributed in the solution. Therefore, we tried to synthesize the ZnS NPs in the presence of Tb^{3+} using a reverse micelles method in which the RE^{3+} ions are confined in a limited space around the ZnS particles, thus energy transfer from ZnS to RE^{3+} can probably be expected. Preparation of the NPs in reversed micelles has been intensively investigated [21,22,26,27] and the variation of particle size can be obtained conveniently by changing the value of $\omega_0 = [H_2O]/[\text{surfactant}]$, the molar ratio of water-to-surfactant. The anionic surfactant sodium bis(2-ethylhexyl) sulfosuccinate (known as aerosol-OT or AOT) is a popular surfactant used to form a thermodynamically stable system (reverse micelles solution) when dissolved in organic solvents. Typically, the radius of the water pool (R_w) follows the relationship: R_w (Å) = 1.5 ω_0 [26].

In this contribution, we report the synthesis of ZnS/Tb^{3+} NPs in different sizes in the presence of Tb^{3+}, as well as Mn^{2+}-doped ZnS NPs prepared using a reverse micelles (water/AOT/isooctane) method for comparison. In addition, we observed the energy transfer from the ZnS host and AOT to trivalent terbium ions, respectively, which are most likely on the surface of nanocrystalline ZnS. The steady-state spectra of both NPs and the surfactant AOT are investigated for better understanding the optical properties of the materials and controlling the preparation processes, which strongly affect the applications of these semiconducting NPs.

2. Experimental

All materials were of analytical grade and were used directly without further purification. Surfactant sodium bis(2-ethylhexyl) sulfosuccinate (AOT) was a white pastelike solid purchased from Fluka. An aqueous solution of 0.1 M zinc chloride with appropriate amount of reactants were made by dissolving $ZnCl_2$ and $TbCl_3 \cdot 6H_2O$ into 50 ml deionized water and keeping the molar ratio of Zn^{2+}/Tb^{3+} to 10/1. Stock solutions of 0.1 M AOT in isooctane and aqueous solution of 0.1 M $Na_2S \cdot 9H_2O$ were prepared, respectively. Reverse micelle solutions containing Zn^{2+}/Tb^{3+} were obtained by adding a mount of stock solution containing Zn^{2+}/Tb^{3+} to 50 ml stock 0.1 M AOT solution, yielding ω_0 values of 10, 14.4 and 20, respectively. Meanwhile, reverse micelle solutions containing S^{2-} were prepared by adding the corresponding amount of the stock $Na_2S \cdot 9H_2O$ aqueous solution to 50 ml as-prepared AOT solutions while keeping the corresponding values of ω_0 unchanged. Equal amounts (50 ml) of reverse micelles solutions with Zn^{2+}/Tb^{3+} or S^{2-}, respectively were then mixed and stirred simultaneously with a magnetic stirrer at room temperature. The sample described as Tb^{3+}/AOT was prepared by adding a mount of Tb^{3+} aqueous solution to 0.1 M AOT stock solution (50 ml) for spectral measurements. For the preparation of ZnS:Mn^{2+} nanoparticles, the Tb^{3+} reactant was replaced by Mn^{2+} from a stock solution containing $ZnCl_2$ and $MnCl_2 \cdot 4H_2O$ (manganese chloride tetrahydrate) in which the molar ratio of Zn^{2+}/Mn^{2+} was 100/1, and the following steps were similar to those described above. The steady-state PL and photoluminescence excitation (PLE) spectra were carried out at room temperature using a Hitachi F-4500 Spectra-fluorometer. Absorption measurements were performed on a Perkin–Elmer model Lambda 9 UV–visible spectrometer, where a micellar solution was used as a reference.

3. Results and discussion

Fig. 1A and B shows the PL and PLE spectra of ZnS:Mn^{2+} and ZnS/Tb^{3+} NPs in water/AOT/isooctane microemulsion, respectively. In the case of ZnS:Mn^{2+} NPs, there are two emission bands in the PL spectrum under the excitation of 290 nm UV light. One is the blue emission band peaking at around 400 nm and the other the orange emission band peaking at 580 nm. It is well known that the blue one is defect-related emission of ZnS, called 'self-activation' luminescence [28], and the orange emission band is originated from $^4T_1$–$^6A_1$ transition of Mn^{2+} inside ZnS NPs. The PLE spectra (monitoring at 580 nm) of the ZnS:Mn^{2+} NPs clearly present

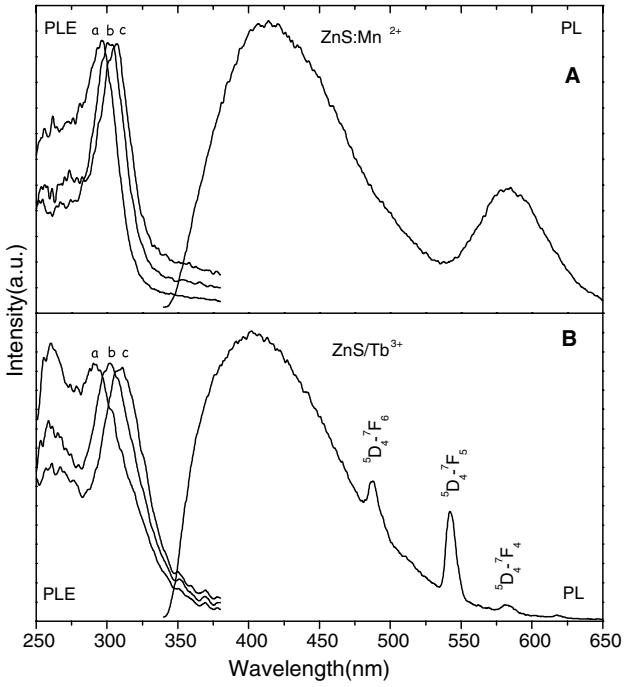

Fig. 1. PL (right, λ_{ex} = 290 nm) and PLE (left) spectra of ZnS:Mn^{2+} (A) and ZnS/Tb^{3+} (B) NPs prepared in water/AOT/isooctane reverse micelles (λ_{em} = 580 nm for ZnS:Mn^{2+} and λ_{em} = 542 nm ZnS/Tb^{3+} NPs in the PLE spectra measurements, a: ω_0 = 10, b: ω_0 = 14.4, c: ω_0 = 20).

a band edge excitation peak of ZnS NPs, which shifts from 307 to 296 nm when reducing particle sizes by decreasing the values of ω_0 from 20 to 10 due to the quantum confinement effect. Hence, one can point out that there is energy transfer from the ZnS NPs to the Mn^{2+} impurities, which gives rise to the orange emission.

In comparison with the spectra of ZnS:Mn^{2+} NPs, the PL spectrum of ZnS/Tb^{3+} under the excitation of 290 nm UV light also presents the broad blue emission band at around 400 nm and a group of sharp lines due to the $^5D_4$–^7F_J ($J = 6, 5, 4, 3$) transitions of Tb^{3+}, in which the $^5D_4$–$^7F_5$ emission at 542 nm is the strongest. The PL excitation spectra of ZnS/Tb^{3+} NPs with various sizes monitored at 542 nm were collected as shown in Fig. 1B. There appear two peaks in each PLE spectrum of the NPs for different ω_0 values. One located around 260 nm is related to AOT, which will be discussed later. The other located around 300 nm is corresponding to the band edge excitation of ZnS NPs in comparison with the PLE spectra of ZnS:Mn^{2+} NPs shown in Fig. 1A. In addition, the absorption edge from ZnS/Tb^{3+} NPs in reverse micelles shifts towards the shorter wavelength side with decreasing ω_0 values as presented in Fig. 2, showing the same trend as the PLE peaks for ZnS/Tb^{3+} NPs with reducing sizes in Fig. 1B due to the quantum confinement effect, and similar reports can be seen in [29] on analyzing the sizes variation of ZnS:Mn^{2+} NPs modified by organic surfactants. Based on the blue shift of absorption edges from 310 to 290 nm, the sizes of ZnS/Tb^{3+} NPs can be estimated to be from 3.0 to 4.5 nm within the framework of effective mass approximation theory [30]. The onsets of absorption (determined by the linear extrapolation of the steep part of the UV absorption curves towards the base line) [31,32] are in conformity with the PL excitation peaks shown in Fig. 1B, which is further indicating that the absorption edges in the range of 290–310 nm are originated from the band edge excitation from ZnS host. Fig. 3 is the PL spectra of ZnS NPs in the presence of different concentrations of Tb^{3+} under the excitation of 290 nm. One can observe the decrease of the ZnS blue band following the enhancement of the Tb^{3+} emission lines with increasing Tb^{3+} concentrations, indicating the performance of energy transfer from the ZnS NPs to Tb^{3+}.

The observation of energy transfer, however, cannot be an evidence of Tb^{3+} being inside the ZnS lattices. Our further experiment indicated that energy transfer from ZnS NPs to Tb^{3+} ions located on the surface of the NPs can effectively occur in a sample prepared by means of mixing two kind of reverse micelles: one only contains ZnS NPs and the other only Tb^{3+} with the same concentrations and values of ω_0 as in the case of preparing ZnS/Tb^{3+} NPs. The mixture sample exhibits nearly the same PL and PLE spectra as those of ZnS/Tb^{3+} NPs (see Fig. 4). Therefore, it can be concluded that an energy transfer between the ZnS NPs and Tb^{3+} can occur across the ZnS/Tb^{3+} NPs interface in water/AOT/isooctane microemulsions.

The PLE peak at 260 nm in ZnS/Tb^{3+} NPs presented in Fig. 1B was also observed in the ethanol [11] or the aqueous system previously [33]. To determine the origin of the 260 nm PLE peak in ZnS/Tb^{3+} NPs, PL ($\lambda_{ex} = 290$ nm) and PLE spectra of AOT and Tb^{3+}/AOT in isooctane were measured and presented in Fig. 5. The emission spectrum of AOT has a band peaking at around 380 nm and the PLE spectrum monitoring at this band shows a broad PLE band peaking at 310 nm with a shoulder at 260 nm. The PLE peak at 260 nm of AOT becomes stronger and dominant in the PLE

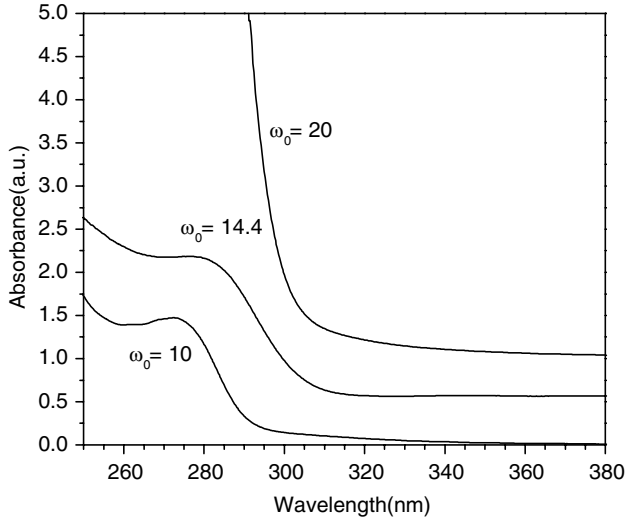

Fig. 2. Absorption spectra of ZnS/Tb^{3+} NPs taken on various values of ω_0 in reversed micelles.

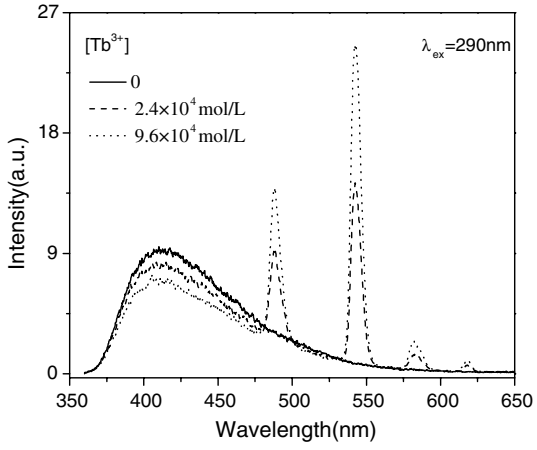

Fig. 3. PL spectra of ZnS NPs with various concentrations of terbium ions which is designated as [Tb^{3+}]. (Tb^{3+}-free ZnS NPs – solid line; 2.4×10^4 mol/L – dashed line; 9.6×10^4 mol/L – dotted line; $\lambda_{ex} = 290$ nm).

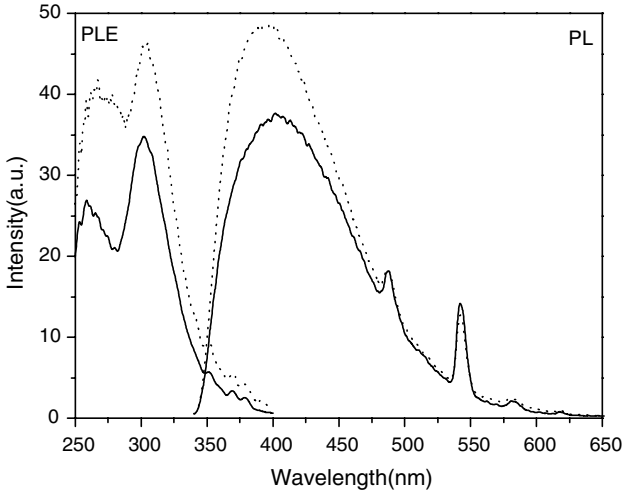

Fig. 4. PL (λ_{ex} = 305 nm) and PLE (λ_{em} = 542 nm) spectra of a mixture of two reverse micelles which one is only containing of ZnS NPs and the other only Tb^{3+}, respectively (solid lines), and those of ZnS/Tb^{3+} NPs in reverse micelles (dotted lines).

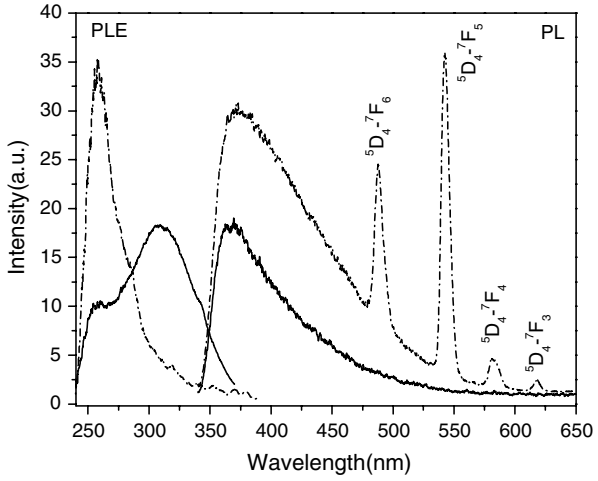

Fig. 5. PL (λ_{ex} = 290 nm) and PLE spectra of AOT (solid lines, monitored at 380 nm) and Tb^{3+}/AOT (dotted lines, monitored at 542 nm) in water/AOT/isooctane reverse micelles.

spectrum of Tb^{3+}/AOT complex, as shown in Fig. 5, indicating the dominant contribution of the 260 nm excitation center to the Tb^{3+} emission lines in comparison with the other excitation center at 310 nm of AOT. Accordingly, the PLE peak at 260 nm in ZnS/Tb^{3+} NPs, as shown in Fig. 1B, is reasonably attributed to the excitation of AOT. Furthermore, it is worth noting that with decreasing the sizes of ZnS/Tb^{3+} NPs, the position of the 260 nm PLE peak keeps unchanged whereas the band edge excitation peak of ZnS NPs shifts to the higher energy side due to the quantum size effects as shown in Fig. 1B. Upon 290 nm excitation Tb^{3+}/AOT gives characteristic emission lines for terbium $^5D_4$–^7F_J transitions, as shown in the PL spectrum in Fig. 5, whereas the absorption due to Tb^{3+} ion itself is negligible. Thus we can argue that there exists energy transfer between AOT and Tb^{3+} ions, and the band around 260 nm can be assigned to the transitions connected with the carbonyl group of AOT molecule through the intra-molecular energy transfer mechanism (IMET) [34].

In the PLE spectra of ZnS/Tb^{3+} NPs (see Fig. 1B), we can also observe that the 260 nm PLE peak grows relatively to the band edge excitation peak of ZnS NPs as the particles size decreases. This behavior can be interpreted as the result of the increase of surface/volume ratio with decreasing NPs sizes, because the number of AOT molecule is proportional to the surface area of the nanosized water pool, and the ZnS molecular number is proportional to the volume of the water pool.

4. Conclusion

ZnS NPs with different diameters have been synthesized successfully using a reverse micelle method in the presence of Tb^{3+}. Both ZnS NPs and AOT molecule can transfer excitation energy to Tb^{3+} ions to emit sharp lines of $^5D_4$–^7F_J transitions. When Tb^{3+} ions are introduced merely on the outside of ZnS NPs in reverse micelles, obvious energy transfer from ZnS NPs to the Tb^{3+} ions is also observed, indicating the important role of spatial confinement on the performance of energy transfer between host and luminescent centers which are even not doped into the host lattices. Reverse micelle is a good confinement environment for obtaining effective energy transfer between host and doped centers in nanometer scaled system.

Acknowledgments

This work is supported by the National Natural Science Foundation of China under Grant Nos. 50172047, 90201010, 10274083 and 'One Hundred Talents Project' of Chinese Academy of Sciences.

References

[1] I. Yu, T. Isobe, M. Senna, J. Phys. Chem. Solids 57 (1996) 373.
[2] C. Tiseanu, R.K. Mehra, R. Kho, M. Kumke, J. Phys. Chem. B 107 (2003) 12153.
[3] T. Kushida, A. Kurita, M. Watanabe, Y. Kanematsu, K. Hirata, N. Okubo, Y. Kanemitsu, J. Lumin. 87–89 (2000) 466.
[4] R.S. Kane, R.E. Cohen, R. Silbey, Chem. Mater. 11 (1999) 90.
[5] W. Chen, V. Zwiller, Y. Huang, S. Liu, R. Wallenberg, J.O. Bovin, L. Samuelson, Phys. Rev. B 61 (2000) 11021.
[6] S.C. Qu, W.H. Zhou, F.Q. Liu, N.F. Chen, Z.G. Wang, H.Y. Pan, D.P. Yu, Appl. Phys. Lett. 80 (2002) 3605.
[7] S.M. Liu, F.Q. Liu, Z.G. Wang, Chem. Phys. Lett. 343 (2001) 489.
[8] W. Chen, A.G. Joly, J.O. Malm, J.O. Bovin, J. Appl. Phys. 95 (2004) 667.

[9] Y. Abiko, N. Nakayama, K. Akimoto, T. Yao, Phys. Stat. Sol. (b) 229 (2002) 339.
[10] L. Sun, C. Yan, C. Liu, C. Liao, D. Li, J. Yu, J. Alloy. Compd. 275–277 (1998) 234.
[11] L. Chen, J. Zhang, Y. Luo, S. Lu, X. Wang, Appl. Phys. Lett. 84 (2004) 112.
[12] M. Ihara, T. Igarashi, T. Kusunoki, K. Ohno, J. Electrochem. Soc 149 (2002) H72.
[13] C. Tiseanu, R.K. Mehra, R. Kho, M. Kumke, Chem. Phys. Lett. 377 (2003) 131.
[14] R.N. Bhargava, J. Lumin. 70 (1996) 85.
[15] A.A. Bol, R.V. Beek, A. Meijerink, Chem. Mater. 14 (2002) 1121.
[16] W.D. Horrocks Jr., D.R. Sudnick, Acc. Chem. Res. 14 (1981) 384.
[17] F.S. Richardson, Chem. Rev. 82 (1982) 541.
[18] M.D. Topal, J.R. Fresco, Biochemistry 19 (1980) 5531.
[19] S. Ravindran, S. Kim, R. Martin, E.M. Lord, C.S. Ozkan, Nanotechnology 16 (2005) 1.
[20] M.E. Akerman, W.C.W. Chan, P. Laakkonen, S.N. Bhatia, E. Ruoslahti, PNAS 99 (2002) 12617.
[21] B.A. Smith, J.Z. Zhang, A. Joly, J. Liu, Phys. Rev. B 62 (2000) 2021.
[22] L. Cao, J. Zhang, S. Ren, S. Huang, Appl. Phys. Lett. 80 (2002) 4300.
[23] W.M. Yen, S. Shionoya (Eds.), Phosphor Handbook, CRC Press, Boca Raton, FL, 1999.
[24] A. Stapor, M. Godlewski, H. Przybylinska, J. Lumin. 40 & 41 (1988) 625.
[25] H. Zhang, Y. Shen, J. Lumin. 40 & 41 (1988) 401.
[26] M.P. Pileni, J. Phys. Chem. 97 (1993) 6961.
[27] M.J. Schwuger, K. Stickdorn, R. Schomacker, Chem. Rev. 95 (1995) 849.
[28] K. Sooklal, B.S. Cullum, S.M. Angel, C.J. Murphy, J. Phys. Chem. 100 (1996) 4551.
[29] T. Kubo, T. Isobo, M. Senna, J. Lumin. 99 (2002) 39.
[30] L.E. Brus, J. Chem. Phys. 79 (1983) 5566.
[31] D.W. Bahnemann, C. Kormann, M.R. Hoffmann, J. Phys. Chem. 91 (1987) 3789.
[32] M. Haase, H. Weller, A. Henglein, J. Phys. Chem. 92 (1988) 482.
[33] N. Murase, R. Jagannathan, Y. Kanematsu, M. Watanabe, A. Kurita, K. Hirata, T. Yazawa, T. Kushida, J. Phys. Chem. B 103 (1999) 754.
[34] I.M. Alaoui, J. Phys. Chem. 99 (1995) 13280.